JOURNAL OF PROPULSION AND POWER
Vol. 18, No. 2, March–April 2002

Slingatron: A High Velocity Rapid Fire Sling

Derek A. Tidman*
Advanced Launch Corporation, McLean, Virginia 22101-1576

The dynamics and mechanics of the spiral slingatron mass accelerator are discussed, together with results from experiments to measure the projectile sliding friction, mass loss, and containment in the curved guide tube used in such a machine. The spiral slingatron appears capable of accelerating a stream of projectiles to very high velocity without overheating the steel guide tube because hot, high-pressure gas is not used. It could derive power from conventional motors such as a turbine that burns kerosene and would fire projectiles without propellant cartridges. The machine has potential applications in areas of industry, defense, impact physics research, and space. Angular dispersion of emerging projectiles can be minimized, but would be larger than for conventional guns. Thus, for some defense scenarios, smart projectiles might be launched that on approach spawn many dumb impactors to shotgun a target. Smart projectiles would also be needed for any gun capable of the long-range missions available due to high launch speed.

Nomenclature

A_p	=	contact area of projectile with track
$A(r)$	=	cross-sectional area of swing arm at r
A_0	=	cross section of swing arm at frame
d	=	tube interior diameter
d_p	=	projectile diameter
F	=	fraction of friction power entering track surface
f	=	gyration frequency, cps
f_{shots}	=	projectiles launched per second
L_{clamp}	=	length of tube enclosed in a clamp
L_g	=	length of tube segment between clamp centers
l_p	=	projectile length
m	=	projectile mass
m_{load}	=	mass carried at the end of a swing arm
P_{nose}	=	gas pressure on front of projectile
q	=	thermal power entering unit area of track
$\langle q \rangle$	=	average thermal power entering unit area of track
R	=	radius of curvature of spiral guide tube
r	=	gyration radius
S	=	design shear strength
T	=	design tensile strength
T_s	=	surface temperature of track
T_0	=	initial temperature of guide tube track
t	=	time
$\boldsymbol{V}$	=	projectile velocity
v	=	gyration speed
α	=	angle between drive plate and swing arm
ΔR	=	gap between neighboring turns of the spiral
ΔT	=	temperature increase of track, $T_s - T_0$
ΔV	=	projectile velocity gain per turn
δh	=	height of rigid projectile midpoint above track
θ	=	angle between gyration velocity and projectile velocity
μ	=	sliding friction coefficient of projectile
ρ	=	density of steel
ρ_p	=	average mass density of projectile

Introduction

A MECHANICAL mass accelerator concept called a slingatron has been proposed and computer models developed for the dynamics of both spiral and circular versions of this machine.[1–7] Here, we first summarize the dynamics of the spiral slingatron in which a projectile (or stream of projectiles) could be accelerated to high velocity. A new approach to the mechanical design of these machines is then discussed together with some potential applications.

The dynamics of the spiral slingatron are similar to whirling a mass around at the end of a string as in a conventional sling (Fig. 1), but with the string growing in length at a constant rate $\dot{R} \ll V$ and with a constant whirling frequency f, cycles per second, so that the projectile moves along a spiral path with an increasing speed $V = 2\pi Rf$. Point A in Fig. 1 is pulled with a constant speed $v = 2\pi rf$ around the inner circle of radius r so that the input power is $\cong v \sin\theta (mV^2/R)$. If the string is massless and inelastic and the projectile moves without friction, it follows from its equation of motion that it gains a constant velocity per turn $\Delta V = 2\pi v \sin\theta$. The angle θ locks into a constant stable value due to the dependence of the aforementioned power input on θ, and the increase of the string length per cycle is $\Delta R = 2\pi r \sin\theta$.

This classical sling has two attractive features. First, it is stable in that the relative phase angle θ between v and V remains approximately constant as the projectile moves out along its spiral path. Second, the velocity gain per turn can be large. For example, $\theta = \pi/3$ gives $\Delta V \sim 5.4v$, so that choosing $v = 200$ m/s would give $\Delta V \sim 1$ km/s/turn, or, for a more extreme case, $v = 1$ km/s, $\Delta V \sim 5.4$ km/s/turn. Unfortunately, any known string would break under the continuously growing tensile stress before V exceeds $\sim$1 km/s.

The spiral slingatron solves the aforementioned string-breaking problem. It consists of a spiral steel tube (Fig. 2) used to guide the projectile along a spiral path as in the aforementioned classical sling. The guide tube is mounted on swing arms distributed along it, so that the entire tube can be propelled and gyrates around a small circle of radius r with a constant gyration frequency f. Work is done on a projectile because the accelerator tube is continually pulled inward at the projectile location against the centrifugal force of the projectile. As the projectile swings out into turns of increasing radius R, it also maintains phase stability with the small-radius gyration of the entire tube. This phase locking is similar to the classical sling in Fig. 1 and enables the projectile to move out around the spiral turns with a constant frequency f, so that its increasing velocity V approximately equals $2\pi Rf$. The device can be viewed as a mass cyclotron.[2]

However, there is a fundamental difference between the classical sling and the slingatron in that there is no string to break under tensile stress in the slingatron. Instead, the guide tube can contain the projectile to much higher speeds because the mechanical impulse per unit length delivered to the tube, $mV/R \cong 2\pi mf$, is approximately constant along the spiral. The tube wall thickness can, thus, remain constant along the spiral.

Received 18 June 2001; revision received 15 October 2001; accepted for publication 29 October 2001.

*President, 6801 Benjamin Street. Senior Member AIAA.

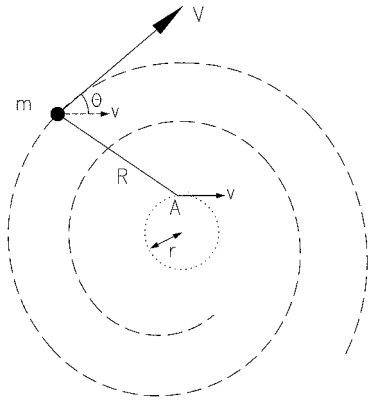

Fig. 1 Classical sling in which the string at point A is pulled with speed v around a circle of radius r with a constant cycling frequency f, and the string grows in length at a constant rate $\dot{R}$.

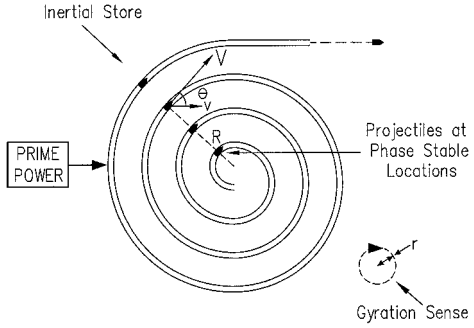

Fig. 2 Spiral tube mounted on distributed swing arms (not shown) that propel the entire spiral around a small gyration circle of radius r at speed v with a constant frequency f cps and the rotation sense shown. The spiral gyrates but does not spin. Projectiles fed into the spiral entrance (at a maximum rate of one per cycle) are pushed forward at v by the closed breech and accelerate through with a stable phase angle θ and increasing speed $V = 2\pi Rf$.

Note that if one treats the tube as an elastic beam clamped at intervals on swing arms, the driving force per unit length in the beam deflection equation swept by a point mass m would be $(mV^2/R)\delta(x - Vt)$ which $\rightarrow 2\pi mf\delta(t)$ as $V \rightarrow \infty$, that is, a uniform impulse for segments traversed with $V \gg$ transverse wave speeds. The projectile wave drag due to the elastic response of the track is also small for all speeds.

Experimentally, we have repeatedly fired 0.738-g lexan projectiles at velocities ranging up to 5.2 km/s into curved 1020 steel tube (o.d. = 0.5, i.d. = 0.3, wall thickness of 0.1 in.) and a radius of curvature $R = 30$ in., so that a force of up to 2.7 tons sweeps around the tube with a contact bearing pressure of 1.37 kbars, with no discernable effect except to smooth slightly the tube asperities. A static force of this magnitude would permanently deform the tube.

For small slingatrons, a single conventional motor could be used to power the gyration, and for larger systems distributed motors could be used to swing the spiral around its gyration circle and continuously supply energy globally to the spiral for extraction by an ongoing stream of projectiles passing through the spiral. The launcher could be operated as a rapid-fire device with a maximum shot frequency equal to the gyration frequency f (assuming the prime power is available), and for a given design its system mass scales approximately[5] in proportion to mV^2.

No gun injector is needed. A projectile inserted into the spiral entrance with the breech closed behind it can accelerate through the spiral. It acquires its initial speed when the breech end moves forward, so that the projectile initial speed (acquired from the breech block) is the same as the gyration speed $v = 2\pi rf$. In this case, it is also necessary for the first turn of the spiral to have a radius of curvature that is no more than a few times the gyration radius and an i.d. slightly larger than the projectile diameter, so that the projectile can negotiate the first turn. A mechanical feed of projectiles into the entrance can then maintain the supply of projectiles.

Note also that the absence of hot propellant gas in the guide tube would allow a higher velocity, projectile mass, and fire rate than conventional guns without overheating the guide tube. Although the spiral guide tube is long, it could be constructed from segments with tapered entrances at the connections. The machine is not sensitive to the exact shape of the spiral, which could approximate an Archimedes spiral.

The two basic issues involved in construction of a slingatron are the sliding friction coefficient of the projectile (with its attendant mass loss) and the implementation of the mechanical system needed to propel the gyration.

Approximate Relationships for the Dynamics

The approximate equations listed here are useful for guideline purposes as a supplement to the computer models based on more exact equations. Computer solutions of the exact equations of motion for a projectile in a gyrating evacuated spiral tube were referred to in Sec. III of Ref. 2, and these results are in agreement with the recent more detailed studies by Cooper et al.[6] and Bundy et al.[7]

An approximate equation of motion for the projectile in a spiral slingatron can be obtained (Fig. 2) by equating the rate of energy gain for the projectile, $(\partial/\partial t)(0.5mV^2)$, to the power used to pull against the projectile centrifugal force, $(mV^2/R)v\sin\theta$, minus the power dissipated by the projectile sliding friction, $\mu mV^3/R$. Note, all three of these powers neglect higher-order terms in the small quantities r, v, and μ, and for this discussion, we also assume that the projectile mass m is constant. The result is

$$\dot{V} \cong (V^2/R)(vV^{-1}\sin\theta - \mu) \tag{1}$$

where R is the guide tube radius of curvature at the projectile location, V the projectile speed in the spiral tube, v the constant gyration speed (assumed $\ll V$), and θ the phase angle between the vectors $\boldsymbol{v}$ and $\boldsymbol{V}$. Projectile drag due to residual gas in the guide tube is neglected in Eq. (1) and is discussed later. We consider only spirals for which the gap between neighboring turns is a constant.

We see from Eq. (1) that the key to achieving a high projectile velocity is to implement mechanically a high gyration speed v and for the projectile to have a small coefficient of sliding friction and to lose only a moderate amount of its mass to supply the gas film on which it slides.

When the exact equations for the dynamics are solved numerically,[2,6,7] one finds that for most of the range $0 < \theta < \pi/2$ stable solutions exist and that the projectile advances with an angular frequency V/R approximately equal to $v/r = 2\pi f$, that is, acceleration occurs. Provided the friction term μ remains smaller than $v\sin\theta/V$ (e.g., because μ decreases with increasing V), the angle θ undergoes only small oscillations about (and a small cumulative displacement in) its stable value to accommodate changes in the relative magnitudes of the Coriolis and friction terms. Phase locking occurs (Fig. 2) because, if a perturbation causes the projectile to move too fast, θ decreases and the gyration velocity component perpendicular to the tube at the projectile location decreases (as does the rate at which work is done against its centrifugal force) and the projectile falls back. Conversely, if it moves too slowly, its relative phase θ increases so that the projectile experiences a larger accelerating force and catches up. Computer models and analysis show that friction damps oscillations about the stable relative phase as the projectile advances through the spiral.

As long as this situation prevails, and acceleration continues, it suffices to assume

$$V/R \cong 2\pi f = v/r \tag{2}$$

For a spiral with constant gaps ΔR between turns, the velocity gain per turn ΔV is also approximately constant,

$$\Delta V \cong 2\pi(v\sin\theta - \mu V), \qquad \Delta R \cong 2\pi(r\sin\theta - \mu R) \tag{3}$$

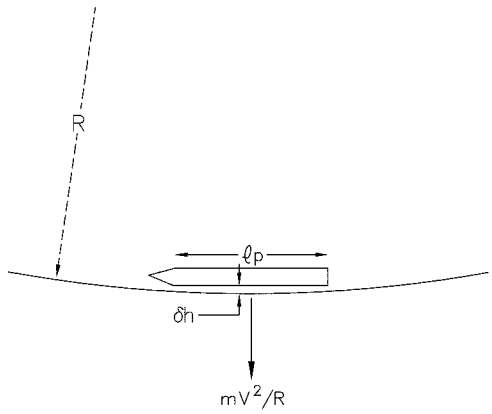

Fig. 3 Rigid projectile traveling along a curved path.

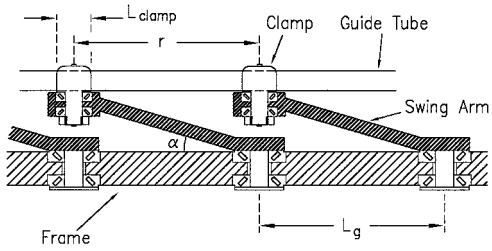

Fig. 4 Swing arms shown oblique to the spiral plane for close packing along the tube; they could also be in pairs above and below the spiral.

and the relative phase θ changes slightly to accommodate changes in μ, provided μ is small.

Finally, note that the guide tube has a radius of curvature R that goes from R_{in} for the inner turn to R_{out} for the outermost turn. If the projectile consisted of a perfectly rigid cylinder of length l_p, it would be supported in the tube on its two ends with its midsection above the tube surface a small height δh given approximately by $l_p^2/8R$ (Fig. 3). However, δh becomes sufficiently small after passing through the first one or two turns, and the centrifugal force becomes sufficiently large that projectile elasticity provides the small amount of flexure (below its elastic limit) needed to push it into tight contact with the tube along the projectile length. As the projectile travels farther out through the spiral, its flexure decreases as R increases, and it could be reduced to zero at exit by gradually straightening out a segment of tube and decreasing its i.d. to fit the projectile diameter just before the exit.

Mechanical Design

The slingatron is subjected to two kinds of stress,[8,9] namely, quasistatic stresses due to gyration and a traveling impulse due to the projectile. Impulsive stresses can be treated approximately using an energy method, or by using detailed codes. In this section, we briefly discuss only the gyration machinery and leave a safety margin so that a range of applicability that includes the traveling impulse of the projectile could be experimentally determined.

To swing the entire spiral around its gyration circle of radius r, the guide tube is attached to swing arms via clamps that turn on tapered roller bearings, as shown in Fig. 4. These bearings allow the entire spiral to roll around its gyration circle while keeping its orientation the same, that is, it gyrates but does not spin. The swing arms could be oblique to the gyration plane of the spiral tube, which allows them to be spaced more closely along the tube without mutual collision occurring, which in turn allows a higher swing speed without shear of the guide tube. Close packing of the clamps also avoids resonance between the gyration frequency f and transverse elastic vibrations of the tube segments. For example, in Fig. 4 they are shown spaced so that the tube segment length between the centers of adjacent clamps is $L_g = r$.

Swing Arms and the Potential for High Gyration and Projectile Speeds

We consider the case in which the arms in Fig. 4 swing in a plane, that is, $\alpha = 0$, which can also be viewed as an approximation for long swing arms with a small finite value for α. The arms then experience tensile stress that remains approximately parallel to a swing arm as it swings around the gyration circle. If we choose to use 4340 (Q&T, 315C) steel for the arm, a design strength of $T = 120{,}000$ psi could be assumed, which is approximately its fatigue endurance limit for cycled stress (even though this stress is not cycled). This allows some added strength for the traveling impulse delivered by the projectile sweeping around the spiral.

If we design the arm with a cross-sectional area A that decreases going away from the frame (Fig. 5) so that its tensile stress T is constant in the arm (i.e., there is no parasitic mass being carried in the arm material itself), we find the result

$$A(r) \cong A_0 \exp(-2\pi^2 \rho f^2 r^2 T^{-1})$$

$$v \cong (2T\rho^{-1})^{0.5}[\ell n(A_0/A)]^{0.5}, \qquad m_{\text{load}} = AT/(4\pi^2 r f^2) \quad (4)$$

where A_0 is the tapered arm cross section at the frame, $A(r)$ the arm cross section at the load, v the swing speed at radius r, and m_{load} the mass (consisting of tube segment, clamp, bearings, and steel to retain the bearings) that can be carried at the end of the arm. Here, $(2T/\rho)^{1/2} \cong 465$ m/s.

However, the clamps and guide tube experience stresses that are both cycled and in the shear direction, so that more complicated geometrical factors are involved in their stress distributions. For these components, we might choose a design strength $S = 60{,}000$ psi for 4340 steel.

Consider the maximum average shear stress at the clamped ends of a tube segment of length $(L_g - L_{\text{clamp}})$ between clamps of length L_{clamp} and density ρ propelled around a circle of radius r with a frequency f. This stress is $\rho v^2 (L_g - L_{\text{clamp}})/2r$, so that the maximum speed (meters per second) with which a uniform tube segment can swing around is

$$v(\max) = [2Sg_E r/\rho(L_g - L_{\text{clamp}})]^{0.5}$$

$$= 320[r/(L_g - L_{\text{clamp}})]^{0.5} \text{m/sec} \quad (5)$$

Here, we used $g_E = 981$ cm/s^2, $\rho = 8$ gm/cm^3, and could allow the clamp to be tapered and extend a length L_{clamp} along the tube for tube support so that the tube segment effective length shown in Fig. 4 is reduced.

In summary, we see that very high swing speeds are possible. For example, for $v = 300$ m/s the projectile velocity gain per spiral turn follows from Eq. (3) as $\Delta V = 1.6$ km/s/turn, neglecting friction and assuming a phase locked angle $\theta = \pi/3$. Conceivably, a future machine using advanced materials (in a reduced pressure environment) might achieve a swing speed of $v = 1$ km/s, in which case $\Delta V = 5.4$ km/s/turn, that is, $V = 21$ km/s in four turns. However, a first-generation machine is likely to operate in the range $v \sim 200$ m/s.

There will be some binding of the motion due to clamping of the tube at multiple locations, but as the spiral gains speed the centrifugal

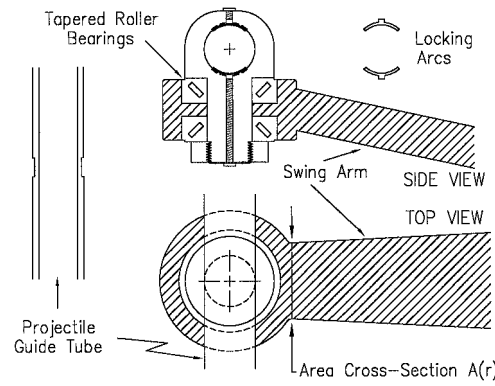

Fig. 5 Tapered swing arms.

forces rapidly become dominant as the tube pulls outward against the swing arms, as was found in a small circular machine.[2]

Reciprocating Machinery for Synchronous Drive

It is important to ensure that the long spiral guide tube swings around its gyration circle synchronously with the swing arms parallel to each other. Although stiffness of the guide tube will contribute to this, additional mechanical methods or electrical feedback control of the distributed drive motors would be needed for multiturn systems. Here we discuss only one of several approaches to synchronization.

Consider the case of a single swing arm with its shaft bearing anchored in a drive plate as shown in Fig. 6a. If the drive plate is propelled in a small radius circular motion, energy can be pumped into the swing arm rotational motion. This swing arm motion can be stably phase locked with the drive plate motion, just as for a conventional sling (in which one's hand replaces the plate), or for a projectile accelerating in a gyrating spiral as discussed earlier.

Thus, if a number of such swing arms were anchored in a drive plate as in Fig. 6b, they could all be synchronously accelerated (once started) by a small-amplitude circular motion of the drive plate, regardless of possibly differing masses and swing arm lengths. This phase stability allows a complete spiral guide tube, clamped by distributed swing arms as in Fig. 6c, to be accelerated up to a high gyration speed while maintaining synchronization along the guide tube length. Guide tube stiffness suffices to start the motion of the spiral in a synchronized state, and phase locking maintains it thereafter.

Another way to view this is to regard Fig. 6a as simply an example of a small mass orbiting about a larger mass, with the two masses tied together by a swing arm. Assume for the moment that the system is not being driven and that the drive plate is confined to slide in a plane with frictionless bearings at its four corners. These two masses then cycle around each other in a plane as the end of the swing arm moves around a circle of radius r, and the heavier plate moves around a smaller circle of radius δr. These radii are independent of the gyration speed, and although the centrifugal forces can become large, they are balanced and distributed internally in the coupled system, just as for a top spinning about its center of mass.

Figures 7 and 8 show an example utilizing this drive principle in which a single automobile engine is used to power the small-amplitude drive plate motion. The drive plate is captured at its four corners by bearings that constrain its motion to a horizontal plane. This restraint involves a relatively small oscillating vertical force (moment) due to the drive plate and the guide tube cycling in planes that are slightly displaced from each other. Two camshafts propel the circular motion of the drive plate, but do not experience the large internal centrifugal forces, provided that they push the drive plate around a circle of radius equal to the natural cycling radius of the drive plate.

The system is essentially a two-stage sling. The cams at the ends of the two vertical shafts in Fig. 8 propel the drive plate around a small circle, and the drive plate, in turn, slings the spiral around a larger circle. The spiral slings the projectile around an even larger radius path with very high speed. All three of these motions occur

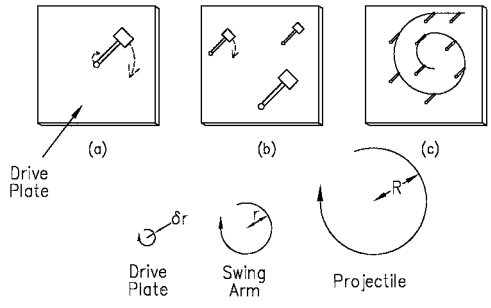

Fig. 6 Stable synchronization of swing arms propelled by the small-amplitude circular motion of a drive plate.

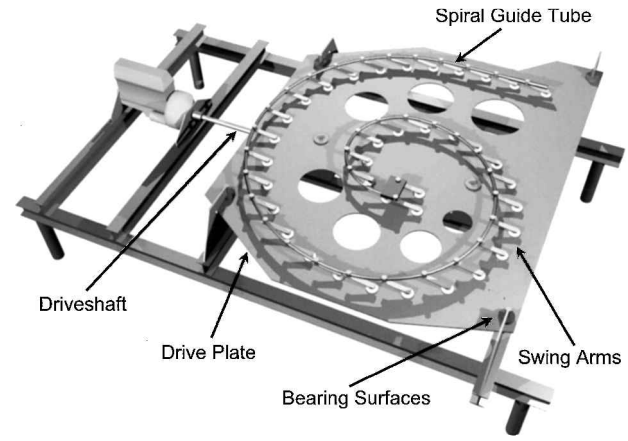

Fig. 7 Conceptual sling powered by an automobile engine via camshafts that power the drive plate.

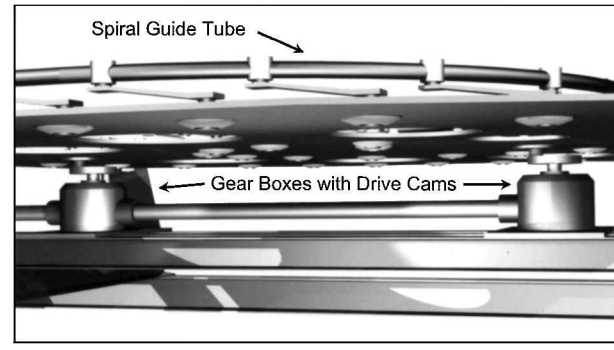

Fig. 8 Side view of the system shown in Fig. 7.

at the same frequency, but with ascending velocities, and the sling motions are phase stable.

Role of Air Drag for High Velocity

The swing arms, guide tube, clamps, etc., experience aerodynamic drag as they swing around the gyration circle at speed v. In addition, the projectile will snowplow air (and, in rapid-fire cases, also bearing gas) in the guide tube, but this could be vented through slots on the inner side of the curved tube as shown in the table top machine in Fig. 4 of Ref. 2.

For a rapid-fire system, the power inputs required to drive the system typically have relative magnitudes: (power to maintain projectile kinetic energy stream) > (aerodynamic swing–drag power) > (roller bearing friction power of drive modules). This assumes a drag coefficient $C_D \sim 1$ for the arms, clamps, and guide tube and also assumes that the fire rate is $> 0.1f$. Although one could reduce the swing drag by streamlining the design of the gyrating components to reduce C_D, this might not be worth doing for the case of a rapid-fire system because the prime power input required is, in any case, dominated by the kinetic energy power required by the projectile stream.

For spirals designed for extremely high projectile velocity, one could eliminate air drag by enclosing the entire system in a reduced-pressure environment. These involve long tapered swing arms with high swing speeds. Figure 9 shows a conceptual four-turn slingatron in a vacuum enclosure that would accelerate projectiles to a velocity $V \sim 21$ km/s if a swing speed $v \sim 1$ km/s could be achieved. Note that the drive plate gyration can be powered from multiple locations because its motion is uniform across the plate, unlike spin that has only one central axis.

Sliding Friction and Mass Loss Experiments

Here, we give a brief summary of experiments described more fully in Ref. 10. Figure 10 shows the layout of the experiment used to obtain data for the projectile velocity loss and mass loss due to

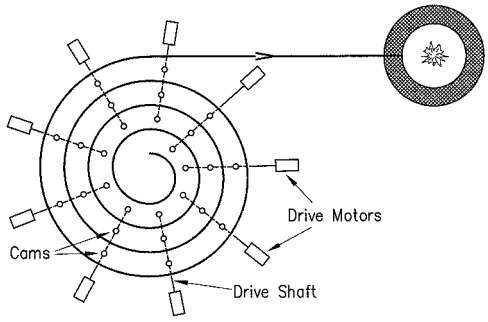

Fig. 9 Conceptual four-turn slingatron in a vacuum enclosure (not shown) with distributed motors powering a drive plate; projectile speed after four turns would be $V \cong 21.6v$, where v is the swing speed.

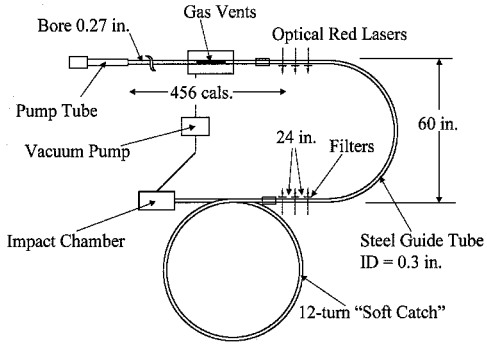

Fig. 10 Layout of experiment to measure projectile sliding friction, mass loss, and containment in a curved guide tube.

friction up to ~4 km/s. It consists of a two-stage light gas gun of small bore size, namely, 0.27 in., that fired lexan projectiles of mass 0.738 g into evacuated semicircular guide tubes of various radii, after which the projectile came to rest in a 12-turn ring that functioned as a soft catch. Figure 11 shows the experimental facility.

The laser triplets located at the input and output ends of the semicircular guide tube provided a measurement of the projectile velocity V_{in} going into the curve and V_{out} leaving the curve. As the projectile passes through the semicircle, it is pushed against the outer wall of the tube, which results in a frictional force $-\mu m V^2/R$. In Fig. 12, we plot data for the quantity $\pi^{-1}\,\ell n(V_{\text{in}}/V_{\text{out}})$ as a function of the average velocity, $0.5(V_{\text{in}} + V_{\text{out}})$ around the semicircle, and in all cases the velocity loss $V_{\text{in}} - V_{\text{out}}$ was small compared with V_{in} . The relationship of $\pi^{-1}\,\ell n(V_{\text{in}}/V_{\text{out}})$ to μ follows from Eq. (1) (with $v = 0$), but is generalized to include a drag term due to bearing gas accumulated on the projectile nose and also to allow for projectile mass loss. Converting the time derivative $\partial/\partial t$ to $V\partial/\partial x$ and integrating along the projectile path around the semicircle then gives

$$\pi^{-1}\,\ell n(V_{\text{in}}/V_{\text{out}}) = \mu - (2\pi)^{-1}\,\ell n(m_{\text{in}}/m_{\text{out}}) + 0.25\pi d^2 R\left\langle P_{\text{nose}}\Big/(mV^2)\right\rangle \tag{6}$$

where the subscripts in and out indicate the projectile velocity or mass either entering or leaving the semicircular tube section, d is the projectile diameter, R is the radius of the semicircular tube, P_{nose} is the reverse pressure from the dusty gas mass that accumulates on the projectile nose, and $\langle\,\rangle$ represents an average value of the argument integrated around the semicircle. The left side of Eq. (6) is the quantity plotted in Fig. 12, and it is only equal to the friction coefficient in the limit that there is zero ablated mass from the projectile and also zero snowplowed dusty gas accumulated on the projectile nose. Figure 13 shows the mass loss of projectiles that were recovered

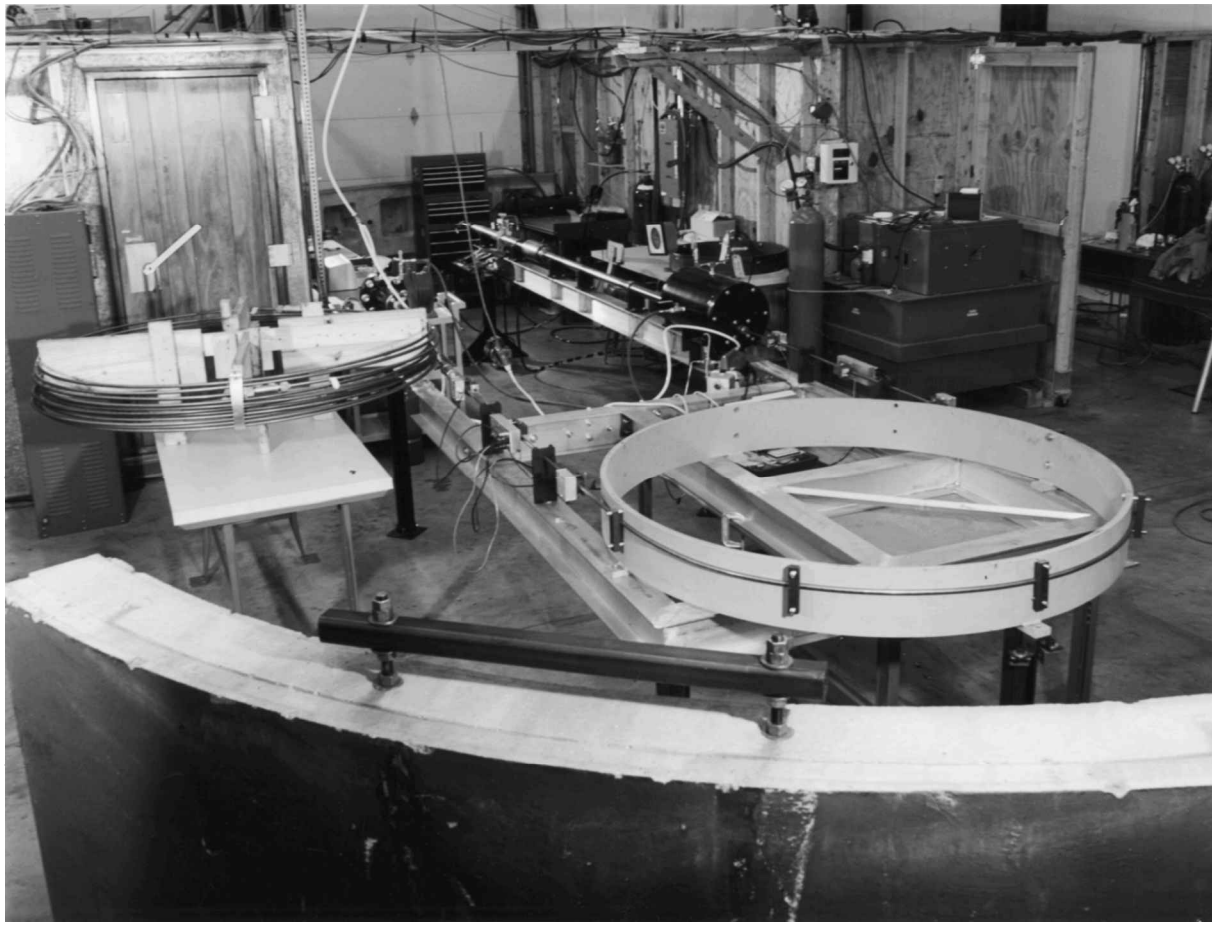

Fig. 11 Experimental facility shown in Fig. 10.

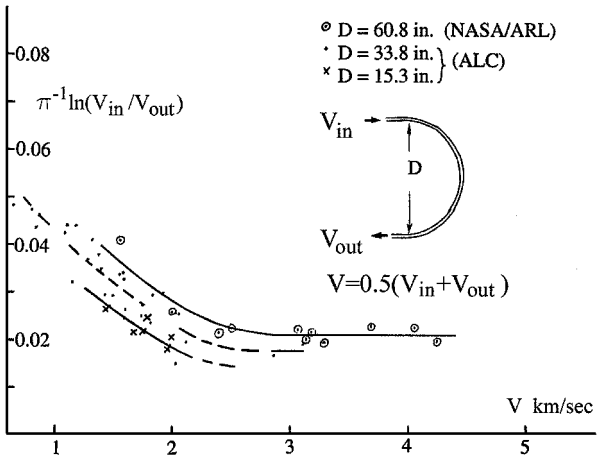

Fig. 12 Velocity-slowing data for 0.738-g lexan projectiles fired through a semicircular arc of steel tube for several values of the arc diameter $D = 2R$. The relationship of the quantity plotted to the friction coefficient is given by Eq. (6).

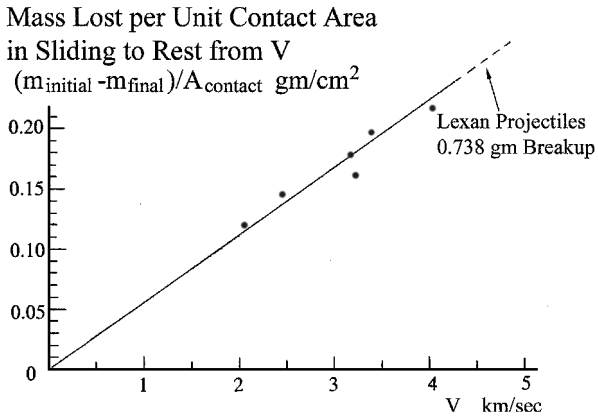

Fig. 13 Mass loss data for 0.738-g lexan projectiles that slide to rest in the multiturn soft catch. For $V_{in} = 3.5$ km/s, about 50% of the 0.738-g projectile had ablated away, and above 4 km/s the projectiles broke up so that data could not be obtained. For a slingatron accelerating these projectiles with a net force α times the frictional drag, one expects α^{-1} times the above mass loss.

from the soft catch. A thin soot film was also generated in the evacuated guide tube by polycarbonate projectiles.

Measurement of asperity heights and microscopic inspection showed that after repeated traversals by lexan projectiles up to ~5 km/s, the track had become slightly smoother and harder, but use of a single 2.4-km/s-Al projectile resulted in shallow gouges.[11]

Potential Defense Applications

Although the slingatron concept is in the design and computer-modeling phase, it would have several advantages if it works as theorized. First, it is a mechanical device that does not involve a flow of high-temperature, high-pressure gas in the guide tube, so that it appears capable of launching large mass projectiles at high velocity and high fire rates without overheating the guide tube.

Second, the accelerating Coriolis force continues to provide projectile acceleration at high speeds, provided the sliding friction coefficient continues to decrease at least as $1/V$ with increasing velocity. Third, the slingatron could be powered by an internal combustion engine, turbine, or electric motor that continuously provides energy to the spiral, which, in turn, directly couples its inertial energy into projectiles passing through the spiral. Finally, the device appears capable of accelerating a continuing stream of smart projectiles through the spiral with a maximum rate limited by the gyration frequency or available power.

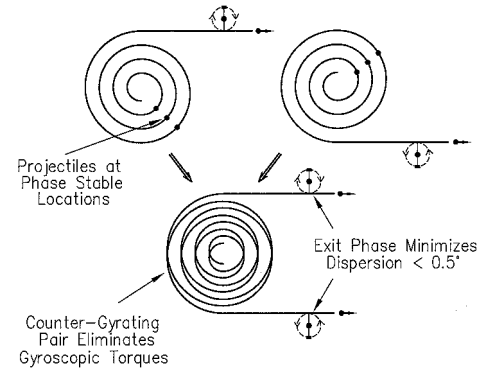

Fig. 14 Two countergyrating spirals that can be redirected as a unit without precession-inducing torques. The linear exit sections are chosen to have a length so that the phase-locked projectiles exit when the swing velocity is parallel to the tube, to minimize angular dispersion at launch.

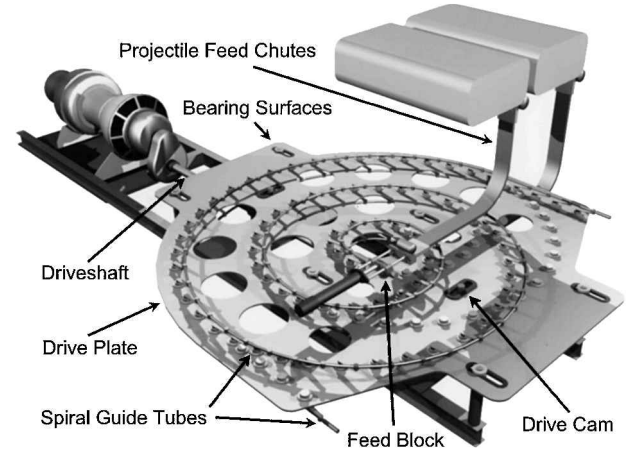

Fig. 15 Conceptual system with countergyrating spirals on opposite sides of a drive plate that executes a small-amplitude linear oscillation powered by a turbine.

Figure 14 shows an arrangement in which two countergyrating spirals are assembled so that as a unit they can be swiveled for aiming without causing precession-inducing torques. Figure 15 shows a concept of a rapid-fire slingatron based on this arrangement in which a turbine powers the system.

The countergyrating spirals shown in Fig. 15 are mounted on opposite sides of a common drive plate structure, and the drive plate would undergo a small-amplitude linear oscillation in response to the pair of countergyrating spirals. Ratchets could ensure that the spirals turn in opposite directions, and the drive plate ensures their locked frequency. Thus, the pair of countergyrating spirals could be brought up to speed by a single high-powered motor that drives a small-amplitude linear oscillation of the drive plate.

Figure 15 also shows an example of a projectile feed system. It consists of a loading block that is propelled by an electrically controlled piston along two rods, on which it executes a linear oscillation with its maximum speed equal to the gyration speed v. The loading block picks up a projectile from a feed chute when the block reaches its maximum amplitude and has zero speed. The loading block then pushes the projectile (past a retaining stop) into the spiral entrance when the block and the spiral are moving adjacent and parallel with velocity v.

Example 1: 0.5-Kilogram Smart Projectiles Launched at 3 Kilometers per Second from a 30-Millimeter Bore Tube

Here we consider a case as in Fig. 15, in which the prime power supply is sufficient to provide a continuous fire rate that might suffice for some missions. For example, assuming a turbine with a shaft power of ~14 MW and a launch efficiency of 50%, the

slingatron could maintain a continuous stream of smart 0.5-kg, 3-km/s projectiles with an average fire rate of $f_{\text{shots}} = 3$ shots/s, which might suffice for some ground-to-air-missions.

An example of a set of numbers for such a machine are swing speed $v = 200$ m/s, frequency $f = 90$ cps, tube i.d. $= 3$ cm and o.d. $= 4$ cm, swing radius $r = 35.4$ cm, final radius of curvature $R = 5.31$ m, velocity gain per turn $\Delta V = 1.09$ km/s, number of turns in the spiral $= 2.75$, projectile diameter $d_p \sim 3$ cm, length $l_p = 28$ cm, and average mass density $\rho_p = 2.5$ g/cm^3. Note, larger f gives a smaller R, for example, $f = 120$ cps and $V = 2.0$ km/s gives $R = 2.67$ m.

Example 2: 50-Kilogram Smart Projectiles Launched at 3 Kilometers per Second

For this larger example, we note that 250-MW turbines exist, for example, in some power generation plants. Assuming the same $\sim$50% efficiency, a single turbine of this power is sufficient to launch a steady stream of 50-kg projectiles at 3 km/s with a continuous fire rate of one per 1.8 s.

Heating of a Spiral Slingatron Tube Used for a Continuous Stream of Shots

Although the slingatron delivers a relatively small thermal load into its guide tube, some heating does occur. We now estimate this heating. In a continuous fire situation, repeated traversals of the track by projectiles will cause the track surface temperature to increase due to projectile sliding friction. Each projectile will impart a thermal pulse to the track and leave in its wake a temperature spike immediately behind the projectile. The track surface then cools as heat diffuses deeper into the tube wall until traversed by another projectile. This process continues and gradually increases the average temperature of the track. However, if this average heating occurs slowly enough, heat can diffuse through the guide tube wall and be removed from the outer surface, by convection, into the air through which it gyrates, in which case further temperature increase of the inner wall ceases. Here, we derive some simple formulas for the spike and average temperature increases of the track and the potential for heat removal for continuous operation of the launcher. The projectiles are assumed to be simple cylinders of length l_p and diameter d, comparable to the i.d. of the guide tube.

The friction power dissipated by a single projectile is $\mu m V^3/R$, where R is the local radius of curvature of the guide tube. This power is shared by evaporation and heating of bearing gas from the projectile contact surface and heating of the track throughout the semicircular contact arc $\pi d/2$ swept out by the projectile. The contact pressure and friction power density are assumed constant throughout the half-cylinder contact surface of the projectile, and a fraction F of this friction power goes into track surface heating.

During a stream of shots, the swept track experiences thermal flux pulses of duration l_p/V and power per unit area q, with a frequency f_{shots}, where $A_p = \pi d l_p/2$ is the projectile contact area. The power density q in a thermal pulse and the average power $\langle q \rangle$ per unit area into the track area swept by repeated traversal pulses are, thus,

$$q = \frac{\mu F m V^3}{A_p R} = \pi \mu F \rho_p d f V^2$$

$$\langle q \rangle = \mu \frac{mV^2}{R} \frac{2F f_{\text{shots}}}{\pi d} = \pi \mu F \rho_p l_p d f f_{\text{shots}} V \tag{7}$$

For the case of a constant heat flux q entering the surface of an infinitely thick slab of material (in this case steel), the heat diffusion equation has a simple solution for the increase in surface temperature $T_s(t)$ over its initial value T_0, namely,

$$\Delta T(\text{K}) = T_s(t) - T_0 = 2qt^{\frac{1}{2}}(\pi \rho_s c_s \kappa_s)^{-\frac{1}{2}} = 0.84 q(\text{W/cm}^2) t_{\text{sec}}^{\frac{1}{2}} \tag{8}$$

where, for steel, the parameters are specific heat $c_s = 0.460$ J/(g $\cdot$ K), density $\rho_s = 7.83$ g/cm^3, and thermal conductivity $\kappa_s = 0.502$ W/(cm $\cdot$ K). Combining Eq. (7) with Eq. (8) gives the temperature spike increase immediately behind a projectile and the average increase in the track temperature of the track after many traversals, namely,

$$\Delta T(\text{spike}) = 0.84 q (l_p/V)^{\frac{1}{2}} = 8.34 \mu F \rho_p f d \left(l_p V_{\text{km/s}}^3\right)^{\frac{1}{2}}$$

$$\langle \Delta T \rangle = 0.84 \langle q \rangle t^{\frac{1}{2}} = 0.0264 \mu F \rho_p d l_p f f_{\text{shots}} V_{\text{km/s}} t^{\frac{1}{2}} \tag{9}$$

where temperature rises are in degrees Kelvin and q in watts per square centimeter. In the final expressions on the right of Eq. (9), lengths, mass densities, frequencies, and times are in cgs units except for the velocities that are in kilometers per second as indicated. Note that f is constant throughout the spiral, so that ΔT (spike) is proportional to $\mu V^{3/2}$ and $\langle \Delta T \rangle$ to μV. If μ decreases with increasing V, then these increases in track temperature become weaker functions of V.

Consider example 1 given in the preceding section, namely, 0.5-kg projectiles launched at 3 km/s at three per second, that is, $f_{\text{shots}} = 3$, and use the slingatron numbers given in example 1. We will also assume that the sliding friction coefficient μ of such large projectiles at $V = 3$ km/s is 0.005 (due to the thicker gas film) and that the fraction of dissipated friction energy going into the guide tube is $F = 0.2$. For this choice, using Eq. (9) we find ΔT (spike) $= 155$ K, and $\langle \Delta T \rangle = 4.49 t^{1/2}$ for which the average temperature would go up by $\sim$142 K after 1000 s, that is, after 3000 shots. Such a slow average heating would have time to diffuse through the tube wall for disposal so that the machine could be operated continuously. However, data are needed for the sliding friction coefficient of larger projectiles.

Finally, from the scaling section in Ref. 5, one can multiply all of the linear dimensions of a given design by the same number, and one has a larger machine that is geometrically similar and as viable mechanically as the smaller machine from which one scaled. However, the temperature increase formulas (9) scale differently. Specifically, as m increases as α^3, the spike temperature increase ΔT behind the projectile increases as α (note $f \sim \alpha^{-1}$), and $\langle T \rangle$ stays the same independent of α provided the shot rate f_{shots} is chosen to be proportional to f. Thus, very large projectiles could also be launched with relatively low thermal energy transfer to the guide tube wall, depending on experimental data for the friction coefficient μ and the fraction F of friction power transferred to track heating.

Summary

The dynamics, mechanics, friction, and thermal physics of the spiral slingatron mass accelerator concept have been discussed, and projectile streams of high velocity appear possible and potentially useful for a variety of industrial, space,[5] and energy applications. Long tapered swing arms provide high swing speeds with lower gyration frequencies. For extremely high projectile speeds, the slingatron could be enclosed in a vacuum environment, and such accelerators might be useful for impact physics experiments including impact fusion using magnetized fuel targets.[12]

If smart projectiles could be manufactured that were cheap and effective, and the machine works as theorized, such systems might also have a useful defense role. Projectiles would not have to individually strike a distant target, but need to be only smart enough to pass close to the target and spawn many small impactors on approach.

Acknowledgments

This work was supported by the Advanced Launch Corporation, including the sliding friction experiment up to 2 km/s using a powder gun. The extension of the friction experiment into the velocity range above 2 km/s using a light gas gun was supported by NASA via U.S. Army Contract/Order DAAD17-00-P-0710, with UTRON, Inc. The author also wishes to thank Paul Westmeyer of the NASA Goddard Space Flight Center, many scientists at the U.S. Army Research Laboratory and UTRON Inc., Mark Kregel, and Jonathan Jones of NASA Marshall Space Flight Center for useful discussions.

References

[1] Tidman, D. A., "Sling Launch of a Mass Using Super-Conducting Levitation," *IEEE Transactions on Magnetics*, Vol. 32, No. 1, 1996, pp. 240–247.

[2]Tidman, D. A., "Slingatron Mass Launchers," *Journal of Propulsion and Power,* Vol. 14, No. 4, 1998, pp. 537–544.

[3]Tidman, D. A., and Greig, J. R., "Slingatron Engineering and Early Experiments," *Proceedings of the 14th SSI/Princeton Conference on Space Manufacturing*, edited by B. Faughnan, Space Studies Inst., Princeton, NJ, 1999, pp. 306–312.

[4]Tidman, D. A., "Method and Apparatus for Moving a Mass in a Spiral Track," U.S. Patent No. 6,014,964, 18 Jan. 2000.

[5]Tidman, D. A., "The Spiral Slingatron Mass Launcher," *Proceedings of the Space Technology and Applications International Forum,* edited by M. S. El-Genk, American Inst. of Physics, Albuquerque, NM, 2001.

[6]Cooper, G. R., Tidman, D. A., and Bundy, M. L., "Numerical Simulations of the Slingatron," *Proceedings of the 10th U.S. Army Gun Dynamics Symposium*, Inst. Advanced Technology, Austin, TX, 2001.

[7]Bundy, M. L., Cooper, G. R., and Wilkerson, S., "Optimizing a Slingatron-Based Space Launcher Using Matlab,"*Proceedings of the 10th U. S. Army Gun Dynamics Symposium*, Inst. Advanced Technology, Austin, TX, 2001.

[8]Harris, C. M., *Shock and Vibration Handbook,* 4th ed., McGraw–Hill, New York, 1996, pp. 9.1–9.13.

[9]Tapley, B. D., *Eshbach's Handbook of Engineering Fundamentals*, 4th ed., Wiley, New York, 1990, pp. 429–569.

[10]Tidman, D. A., "A Scientific Study on Sliding Friction Related to Slingatrons," Advanced Launch Corp. TN 2001-1, Final Rept. U.S. Army Contract DAAD17-00-P-0710, 2001.

[11]Stefani, F., and Parker, J. V., "Experiments to Measure Gouging Threshold Velocity for Various Metals Against Copper," *IEEE Transactions on Magnetics,* Vol. 35, No. 1, Jan. 1999, pp. 312–316.

[12]Lindemuth, I. R., and Kirkpatrick, R. C., "Parameter Space for Magnetized Fuel Targets in Inertial Confinement Fusion," *Nuclear Fusion*, Vol. 23, No. 3, 1983, pp. 263–284.